Device Fabrication and Characterization Techniques for Semiconductor Devices

1.2 Thin Film Deposition Techniques

1.2.1 Sputtering

Sputtering is one of the widely popular technique for depositing transparent conducting oxides [3]. It is widely used to deposit thin films of different materials over different substrates. Its many potential advantages such as low temperature deposition, high uniformity, good adhesion of films over the substrate, ability of depositing many compounds from elemental targets and long-term stability of the process with lower deposition cost makes it highly popular technique for depositing thin films.

When a material in solid form is bombarded by high energy ions at any temperature, the surface atoms of the material may get sufficient energy so that they can come out from the target surface and this process is called as sputtering. The sputtering technique gives highly crystalline films with good uniformity over the large areas. High controllability over various deposition parameters such as sputtering power, gas flow rate and substrate temperature makes it a potential choice in semiconductor manufacturing where mass production with large area deposition is desired. Furthermore, the spitting issues that arise in thermal evaporation for high melting point materials do not occur in sputtering method. Fig.1 and 2 shows the schematic diagram and experimental setup of RF sputtering technique.

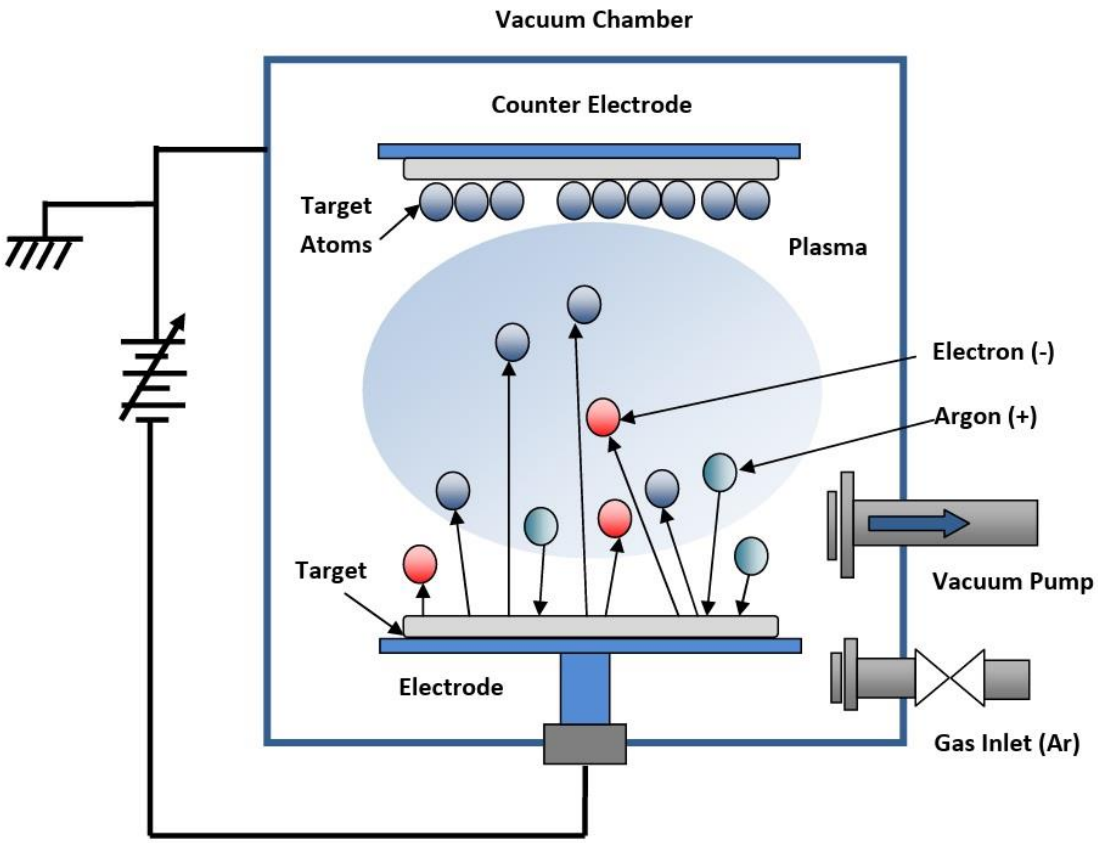

Fig.1 Schematic diagram of RF sputtering technique.

In sputtering process, high energy particles usually inert gases such as argon is used to withdraw the surface atoms from the source material (generally called as sputtering target). Sputtering uses controlled injection of argon in high vacuum environment (generally varying between 10^{-5}-10^{-7}mbar) in order to improve the mean free path of sputtered atoms with high purity and controllability. The high vacuum and controlled argon flow rate is sufficient to support the dense plasma between two high voltage electrodes. When the RF generator is turned on, an electric field gets stabilized between the target and substrate. In first phase of alternate supply, the biasing of the substrate is at higher potential as compared to the target. Under these conditions, any electron present in the chamber due to some background radiations or due to electron ejection from target, accelerates towards the substrate and collides with argon atoms on the way. This collision between high energy electrons and argon atoms results in positive argon ions and additional electrons. These ionized argon atoms are attracted towards the sputtering target in order to withdraw the material particles from target. The secondary electrons generated during this process again accelerate towards the substrate which leads to more collision and ionization. The argon ions which strikes the sputtering target can bounce back, can be adsorbed over the surface, can implant itself into the target or

can remove the target surface ions. The argon ions accumulated over the target surface during this process increases the target potential which results in self-biasing that can hamper the acceleration of other argon ions towards the target. This accumulation of the argon ions over the target surface can be a serious issue in the case of insulating targets. However, the RF supply with quick potential reversal do not allows the ions to get buildup over the surface. In the second phase of the RF supply, the potential of the target become higher than the substrate which results in no deposition and argon ions will move away from the target which will minimize the self biasing. This self biasing is a serious issue in dc sputtering for insulating targets. As a consequence DC sputtering is generally preferred for conducting materials and RF sputtering can be used for depositing semiconductor and non-conductive materials. In RF magnetron sputtering, the magnets near the target increase the electron travel path which results in many more collisions and hence plasma density increases. In addition to this, magnetic fields near the target traps the electrons in its vicinity and keep the electrons away from the substrate which reduces substrate heating and film damage due to high energy electrons. AC current in RF range prevents the self biasing of the sputtering target which enables the deposition of the insulating films too.

Fig.2 Experimental setup of RF sputtering system

3.2.2 Thermal Evaporation:

Thermal evaporation is one of the popular deposition technique in which electrical energy is used to vaporize the solid material by heating it to sufficiently high temperature [4]. In thermal evaporation, a high current is passed through the filament/crucible which is generally made-up of metals like tungsten, molybdenum or tantalum so that it can sustain at very high temperature. The selection of filament/crucible material is dictated by the evaporation temperature and chemical reaction between the material and crucible. Fig.3 shows the schematic diagram of thermal evaporation system. When high electrical current is passed, the material in the crucible gets evaporated and condenses over the substrate in order to form thin film. Generally, low deposition pressure in the range of 10^{-5}-10^{-7} mbar is required to avoid the reaction between the vapor and atmosphere. At lower deposition pressure, the mean free path of evaporated material and vacuum chamber have the same order, so that these evaporated particles travel in a straight line from source to substrate. High vacuum is also necessary condition to obtain contamination free films. Fig. 4 shows experimental setup for thermal vapor evaporation system.

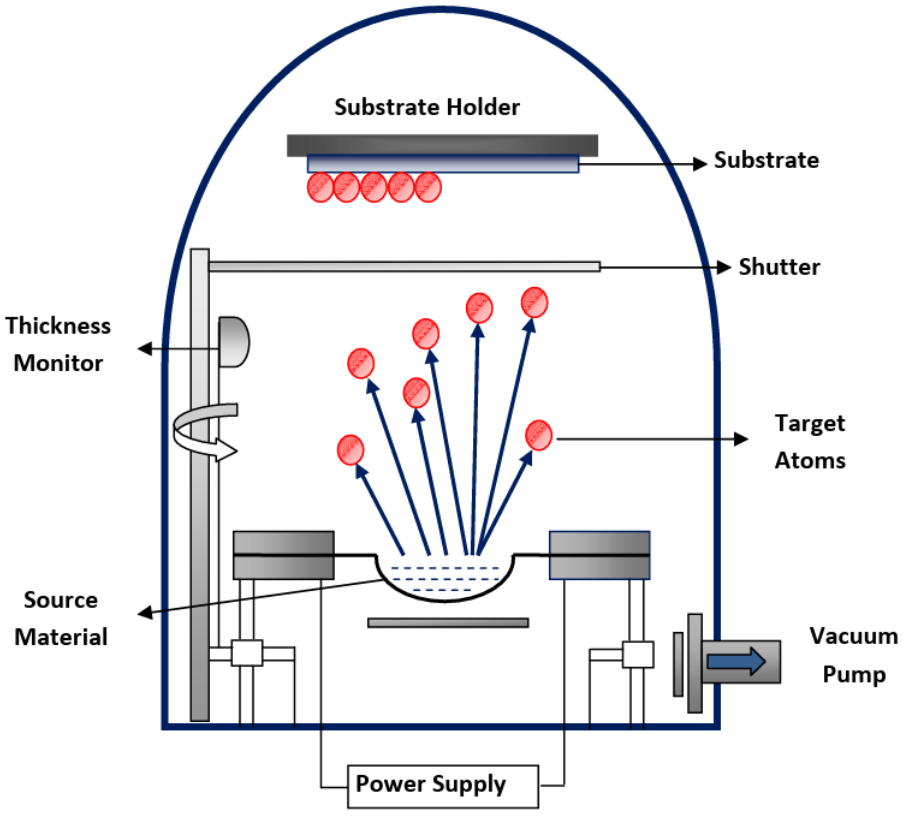

Fig.3 Schematic diagram of thermal vapor evaporation technique.

Fig.4 Experimental setup of thermal vapor evaporation technique (

1.3 Structural and Surface Morphological Measurement Techniques

1.3.1 X-Ray Diffraction

X-Ray diffraction is an important characterization technique to study the atomic spacing and crystal structure of deposited films [4]. A variety of micro structural parameters such as grain size, lattice constants, dislocation density, stress and strain can be derived from XRD data. X-Ray diffraction's basic working principle is constructive interference of crystalline sample and monochromatic X-rays. In XRD, cathode ray tube generates the X-rays which are filtered to produce monochromatic light. This monochromatic light is collimated and directed over the sample. The interaction of X-Ray and sample gives the constructive interference when it satisfies the Bragg's law (i.e. $n\lambda=2d\sin\theta$). Where n is integer, λ is wavelength, d is the inter-plane spacing in the crystal lattice and θ is the angle between incident beam and sample space. The inclined lines shown in Fig. 5 shows the distance between the planes defined using miller indices h, k and l. When X-ray incidents on the sample, it gets reflected from the sample and passes through several slits such as collimator and filter before reaching to the detector. The samples are scanned through all 2θ angles so that all possible diffraction directions due to random orientation of the material can be obtained. These diffraction peaks

obtained from XRD gives the identification of the desired material. The experimental setup of X-Ray diffractometer is shown in Fig. 6. The different microstructural parameters such as crystalline size (G), lattice constants (a, b, c), dislocation density (δ), residual stress (σ) and strain (ε) that can be derived from XRD data are as follows [5]:

$$G = \frac{0.9\lambda}{\beta \cos\theta} \tag{1}$$

$$\delta = \frac{1}{G^2} \tag{2}$$

$$a = b = \sqrt{\frac{1}{3}} \frac{\lambda}{\sin\theta} \tag{3}$$

$$c = \frac{\lambda}{\sin\theta} \tag{4}$$

$$\sigma = -233 \frac{c_{film} - c_{bulk}}{c_{bulk}} \tag{5}$$

$$\varepsilon = \frac{\beta}{4\tan\theta} \tag{6}$$

Where λ is X-ray wavelength, β is full width at half maximum (FWHM), θ is Bragg's angle and c_0 (5.206 Å) is the unstrained lattice constant for bulk ZnO.

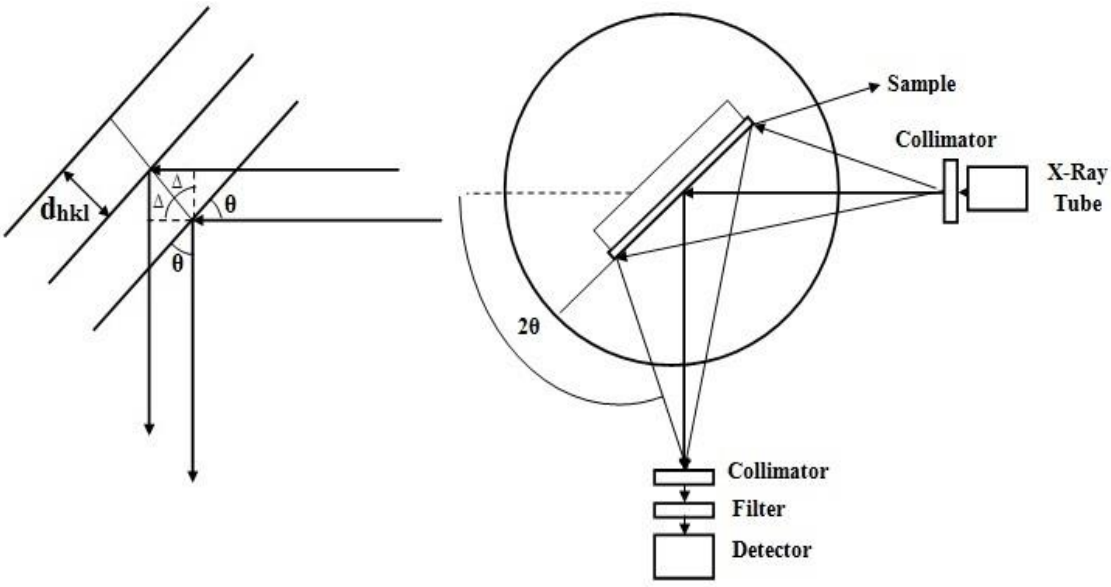

Fig. 5 Basic working principle of X-Ray diffraction technique.

Fig. 6 Experimental setup of X-Ray diffraction system

1.3.2 Scanning Electron Microscope (SEM)

The Scanning Electron Microscope generally produces largely magnified images of deposited films using electrons so that surface morphology of the deposited films can be analyzed [6]. Fig. 7 and 8 shows the basic working principle and experimental setup of SEM. An electron gun at the top of the microscope is used to produce high energy electron beam. The beam travels vertically through the electromagnetic fields and lenses under vacuum to fall over the sample surface. When the focused electron beam strikes the sample surface, X-Rays, secondary electrons and back scattered electrons are ejected from the sample which are collected by detectors and converted into the signals that can be seen at computer screen.

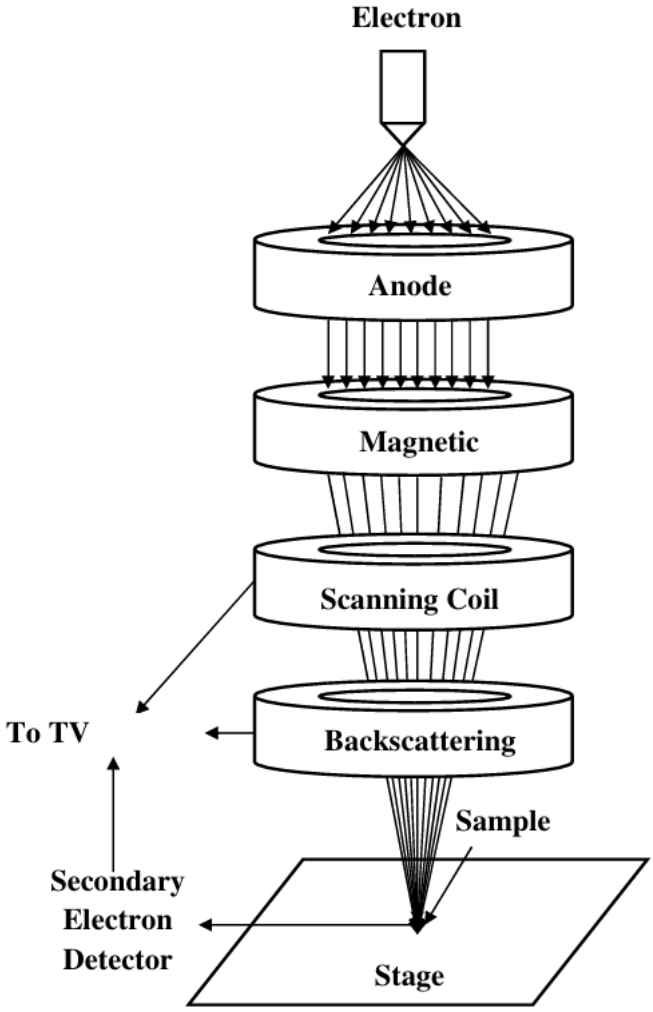

Fig.7 Basic working mechanism of scanning electron microscope.

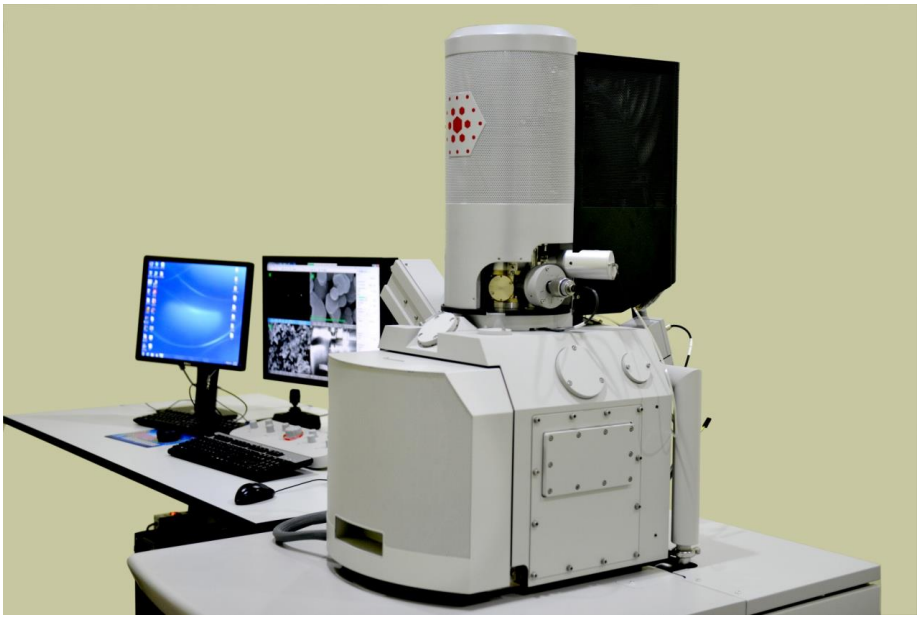

Fig.8 Experimental setup of scanning electron microscope

1.3.3 Atomic Force Microscope (AFM)

The Atomic Force Microscope (AFM) is used to obtain surface forces and images at nano and micro level [6,7]. The basic working principle of AFM is shown in Fig.9. The cantilever spring is attached with standard microscopic tip. The basic working of AFM depends upon the bending of the cantilever spring when some external force is applied. When an adhesive interaction between tip and surface takes place, very sensitive cantilever bending due to surface and tip contact comes into picture. In order to detect this bending, a laser beam from the laser source is focused on the cantilever that reflects from cantilever and reaches towards the position sensitive detector as shown in Fig. 9. Depending upon the deflection of cantilever, the position of reflected laser beam changes. The position sensitive detector senses this deviation and converts this change into electrical signal. The surface imaging of the surfaces in AFM can be done using two measurement methods. (i) Contact Mode (ii) Tapping Mode. In contact mode, physical contact between sample and tip takes place. The electronic feedback maintains the resulting defletion at a constant value by changing the Z position and thus the force is measured. In tapping mode, the cantilever tip is forced to vibrate near resonant frequency. As the vibrating tip approaches the surface, the vibration amplitude of the cantilever will decrease and the interaction force between the tip and the surface will shift the resonant frequency. In tapping mode, the surface is scanned in terms of change in oscillation amplitude. The atomic force microscope can achieve a lateral resolution of 0.1-10 nm. Fig.10 shows experimental setup for atomic force microscope.

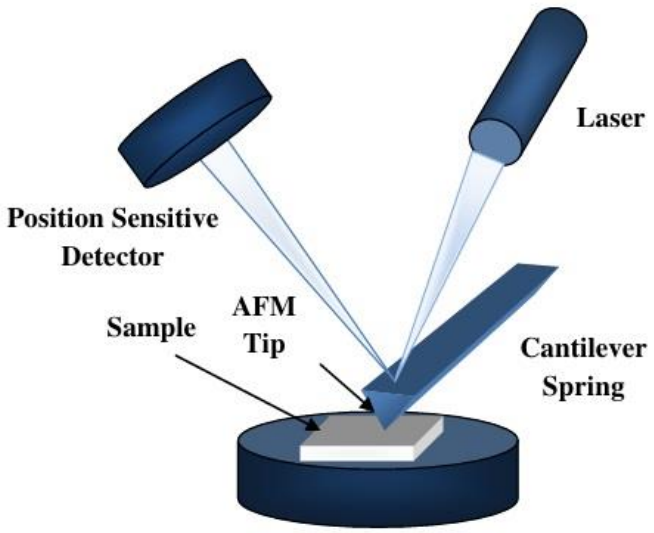

Fig.9 Basic working mechanism of atomic force microscope in contact mode.

Fig.10 Experimental setup of atomic force microscope

1.3.4 Transmission Electron Microscope (TEM):

Transmission electron microscopy is used to obtain detailed images of extremely small areas with a magnification of about 1000 kX using electron beam. TEM can be used to analyze various features such as crystal structure, dislocations and grain boundaries etc [8]. High resolution images obtained from TEM can also be used to analyze shape, size, density and quality of the quantum wells, wires and dots. The experimental setup and basic working mechanism of transmission electron microscope is shown in Fig.11 and 12 respectively. In TEM, the electron beam produced from electron gun is focused into a thin, small and coherent beam using condenser lenses. The condenser aperture is generally used to exclude high angle electrons. The transmitted part of condenser aperture beam strikes to the sample and passes through the sample depending upon the electron transparency and thickness of the sample. The transmitted portion is focused on the phosphor screen using objective lenses. Some optional objective lenses can also be used to improve the contrast by blocking the electron diffraction at higher angles. Further, the image is passed through intermediate and projection lenses so that higher magnification can be achieved.

Fig.11 Experimental setup of transmission electron microscope

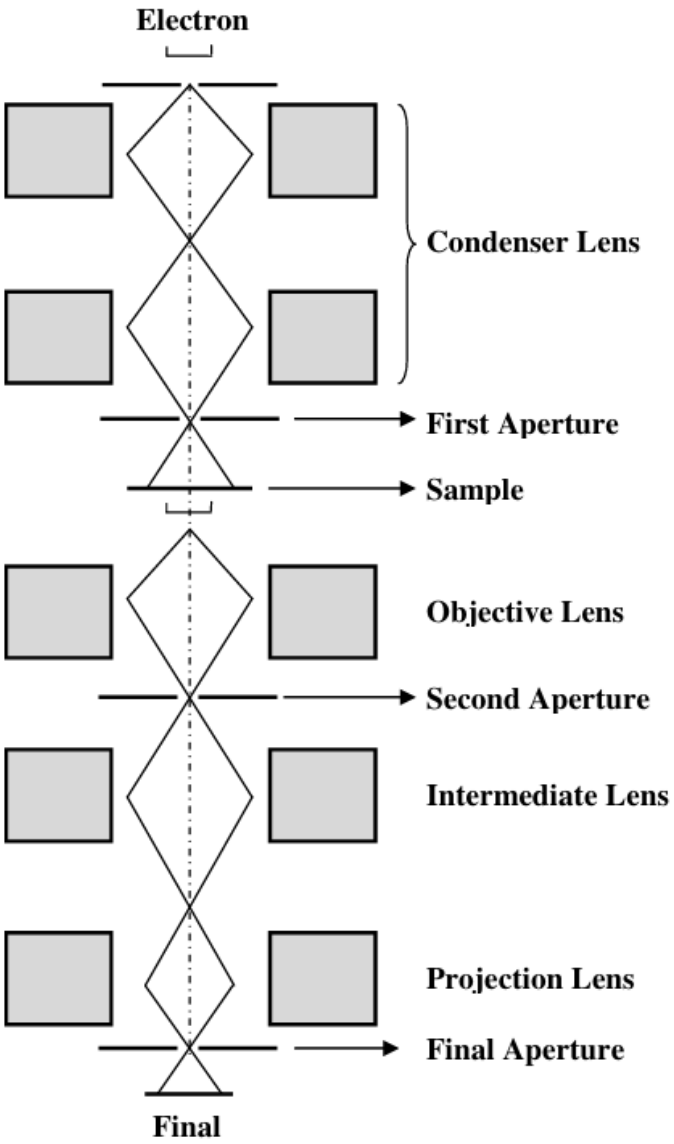

Fig.12 Schematic diagram for basic working mechanism of transmission electron microscope.

1.5 Electrical Characterization Techniques

The electrical properties of heterojunctions are generally studied using current-voltage and capacitance-voltage measurements. The various important device parameters such as ideality factor, barrier height, built-in potential, donor concentration and depletion width can be derived from these measurements.

1.5.1 Current-Voltage Characteristics

Current voltage measurement plays a significant role in order to investigate the performance of various thin film based devices such as solar cells, thin film transistors and different detectors. The values of ideality factor (η) and effective barrier height ($\phi_{B,eff}$) can be obtained using following equations [12]:

$$\eta = \frac{q}{kT} \times \{\frac{dV}{d(\ln I)}\} \tag{18}$$

$$\varphi_{B,eff} = \frac{kT}{q} \times \ln\left(\frac{AA^*T^2}{I_0}\right) \tag{19}$$

Where k is Boltzmann constant, A is contact area, A^* is effective Richardson constant and I_0 is reverse saturation current.

1.5.2 Capacitance - Voltage Characteristics

In semiconductor heterojunctions, the capacitance versus voltage plot is very useful to investigate the charge distribution and depletion region potential. The capacitance versus voltage relation can be explained by conventional heterojunction theory [13]:

$$C^2 = \frac{qN_AN_D\varepsilon_1\varepsilon_2}{2(\varepsilon_1N_D + \varepsilon_2N_A)(V_{bi} - V)} \tag{20}$$

Where N_D is donor density, N_A is acceptor density, ε_1 and ε_2 are dielectric constants of ZnO and silicon respectively, V_{bi} is built-in potential and V is biasing voltage. Considering $V >> kT/q$ and $N_A > N_D$, the depletion region capacitance per unit area for a given reverse bias voltage as a function of permittivity can be written as follows:

$$\frac{A^2}{C^2} = \frac{2(V_{bi} - V)}{q\varepsilon_sN_D} \tag{21}$$

The value of built-in potential (V_{bi}) can be obtained from linear region intercept of A^2/C^2 versus voltage curve towards the biasing voltage axis. The value of donor concentration can be obtained by putting the value of slope in the following equation:

$$N_D = \frac{2}{slope * q\varepsilon_s} \tag{22}$$

Effective barrier height of semiconductor heterojunctions can be obtained as:

$$\varphi_{B,eff} = V_{d0} + \frac{kT}{q}\ln\left(\frac{N_C}{N_D}\right) \tag{23}$$

Where V_{d0} is diffusion voltage at 0V and can be expressed as $V_{d0} = V_{bi} + (kT/q)$. N_C is effective density of states in conduction band. The positions of fermi levels can be calculated using following equations [14]:

$$E_f - E_c = \frac{kT}{q} \times \ln\left(\frac{N_D}{N_C}\right) \tag{24}$$

$$E_V - E_f = \frac{kT}{q} \times \ln\left(\frac{N_A}{N_V}\right) \tag{25}$$

The depletion width of the fabricated p-n junction can be obtained as [15]:

$$W_{Dep.} = \sqrt{\frac{\varepsilon_0 \varepsilon_s (V_{bi} - V)}{qN_D}} \tag{26}$$

(a)

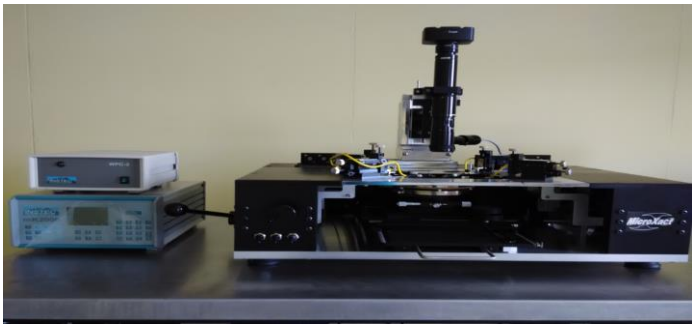

(b)

Fig.17 Setup for I-V/ C-V measurement (a) measuring unit (b) probe station.